Electronic Supplementary Material (ESI) for New Journal of Chemistry.

Supporting Information

Mechanistic understanding of the effect of alloying Au with Ni on N_2 electroreduction into NH_3: theoretical considerations

Lihui Ou*, Peiyu Hu, Yuandao Chen, Junling Jin

1. Model and Computational Details

1.1 Surface and Solvation Model

Low-index (111) crystal facet of Au is chosen as representative surface for present theoretical studies due to experimentally proved high thermal and kinetic stability.[1] Considering the complexity of N_2 electroreduction systems, the electrode/aqueous interface is included in the present study, in which 12 explicit H_2O molecules with two relaxed bilayer structures chosen to fill up the vacuum region were used to model the solvation effect in order to better simulate the interactions among surface, solvent and adsorbates and decrease the size of the simulated systems as much as possible (See Figure S1). In fact, the formation of an ordered H_2O bilayer structure in a hexagonal arrangement with respect to the surface normal had been demonstrated by X-ray absorption spectroscopy, thermal desorption spectroscopy, low-energy electron diffraction, X-ray photoelectron spectroscopy and scanning electron microscopy along with DFT calculations in previous experimental and theoretical studies on the meal surface.[2-4] Our present solvation model is on the basis of the previous studies on structure and orientation of H_2O. However, many different H_2O solvation structures may also exist, which all are approximate in energy.[5] Since all energies of interest in this study are energy differences, which are not sensitive to the accurate model of H_2O as long as the same model is consistently used and a reasonable model in a local minimum structure is choose when calculating the energy differences. Considering different Au/Ni atomic ratios (Au: Ni = 3:1, 1:1 and 1:3), a (4x4) $Au_3Ni(111)$, $Au_1Ni_1(111)$ and $AuNi_3(111)$ slab model with 16 metal atoms per layer and respective theoretical equilibrium lattice constant by using four metal layers was created. The calculated equilibrium

---

**Hunan Province Cooperative Innovation Center for the Construction & Development of Dongting Lake Ecologic Economic Zone, Hunan Provincial Key Laboratory of Water Treatment Functional Materials, Hunan Province Engineering Research Center of Electroplating Wastewater Reuse Technology, College of Chemistry and Materials Engineering, Hunan University of Arts and Science, Changde, 415000, China. E-mail: lihuiou@huas.edu.cn*

lattice constant for bimetallic Au_3Ni_1, Au_1Ni_1 and Au_1Ni_3 alloys is 4.04, 3.88 and 3.71 Å, respectively.

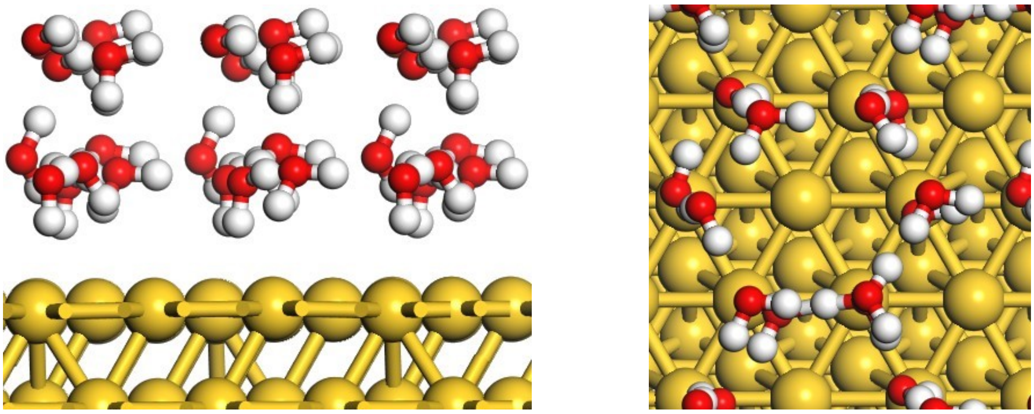
(a) (b)

Figure S1. The solvation model on Au(111) at the electrochemical interface: (a) Side view; (b) Top view.

1.2 Computational Parameters

Using the generalized gradient approximation of the Perdew–Burke–Ernzerhof exchange correlation functional, all calculations were performed in the framework of DFT.[6] The ultrasoft pseudopotentials were employed to describe the nuclei and core electrons and the Kohn-Sam equations were self-consistently solved using a plane-wave basis set.[7] A kinetic energy cutoff of 30 Ry and a charge-density cutoff of 300 Ry were used to make the basis set finite. The Fermi surface has been treated by the smearing technique of Methfessel–Paxton with a smearing parameter of 0.02 Ry.[8] The PWSCF codes in Quantum ESPRESSO distribution were employed to perform all calculations.[9] Brillouin-zone integrations were implemented using a (3×3×1) uniformly shifted k-mesh for (4×4) supercell with the special-point technique, which was tested to converge to a subset of the relative energies reported herein. A vacuum layer of 16 Å was placed above the top layer of slab, which is sufficiently large to ensure that the interactions are negligible between repeated slabs in a direct normal to the surface. The Au and M atoms in the bottom two layers are fixed at the theoretical bulk positions, whereas the top two layers and all adsorbates including solvent are allowed to relax to minimize the total energy of the system. Structural optimization was performed until the Cartesian force components acting on each atom were brought below 10^{-3} Ry/Bohr and the total energy was converged to within 10^{-5} Ry. Using the climbing image nudged elastic band (CI-NEB) method, the saddle points and minimum energy paths (MEPs) were located.[10, 11] Zero point energy (ZPE) corrections were applied into the calculations of activation and reaction energies from MEP analysis, in which density functional perturbation theory within the linear response was used to study the vibrational properties.[12] The ZPEs were calculated using the PHONONS code that contained in the Quantum ESPRESSO distribution.[9]

References

1 L. M. Yang, M. Dornfeld, T. Frauenheim and E. Ganz, Glitter in a 2D Monolayer, *Phys. Chem. Phys. Chem.*, 2015, **17**, 26036-26042.

2 E. Skúlason, V. Tripković, M. E. Björketun, S. Gudmundsdóttir, G. Karlberg, J. Rossmeisl, T. Bligaard, H. Jónsson and J. K. Nørskov, Modeling the Electrochemical Hydrogen Oxidation and Evolution Reactions on the basis of Density Functional Theory Calculations, *J. Phys. Chem. C*, 2010, **114**, 18182-18197.

3 M. A. Henderson, Interaction of Water with Solid surfaces: Fundamental Aspects Revisited, *Surf. Sci. Rep.*, 2002, **46**, 1-308.

4 H. Ogasawara, B. Brena, D. Nordlund, M. Nyberg, A. Pelmenschikov, L. G. M. Pettersson and A. Nilsson, Structure and Bonding of Water on Pt(111), *Phys. Rev. Lett.*, 2002, **89**, 276102.

5 S. Haq, C. Clay, G. R. Darling, G. Zimbitas and A. Hodgson, Growth of Intact Water Ice on Ru(0001) between 140 and 160 K: Experiment and Density-Functional Theory Calculations, *Phys. Rev. B*, 2006, **73**, 115414.

6 J. P. Perdew, K. Burke and M. Ernzerhof, Generalized Gradient Approximation Made Simple, *Phys. Rev. Lett.*, 1996, **77**, 3865-3868.

7 D. Vanderbilt, Soft Self-Consistent Pseudopotentials in a Generalized Eigenvalue Formalism, *Phys. Rev. B*, 1990, **41**, 7892-7895.

8 M. Methfessel and A. T. Paxton, High-Precision Sampling for Brillouin-Zone Integration in Metals. *Phys. Rev. B*, 1989, **40**, 3616-3621.

9 S. Baroni, A. Dal Corso, S. de Gironcoli and P. Giannozzi, PWSCF and PHONON: Plane-Wave Pseudo-Potential Codes, http://www.quantum-espresso.org/, **2001**.

10 G. Henkelman and H. Jonsson, Improved Tangent Estimate in the Nudged Elastic Band Method for Finding Minimum Energy Paths and Saddle Points, *J. Chem. Phys.*, 2000, **113**, 9978-9985.

11 G. Henkelman, B. P. Uberuaga and H. Jonsson, A Climbing Image Nudged Elastic Band Method for Finding Saddle Points and Minimum Energy Paths, *J. Chem. Phys.*, 2000, **113**, 9901-9904.

12 S. Baroni, S. Gironcolli, A. Corso and P. Giannozzi, Phonons and Related Properties of Extended Systems from Density Functional Perturbation Theory, *Rev. Mod. Phys.*, 2001, **73**, 515-562.